Developing a 3U CubeSat Engineering Model - FlatSat & Chassis Design

William Crofts[1], Mattias Langer[2], Alex Bolland[2], Tahrim Uddin[2], Chiara Biquet[2], Eduard Hopkins[2], Jai Bassi[2], Myles Ing[2], Julia Hunter-Anderson[2]

Abstract
WUSAT-3 is a 3U CubeSat being designed to carry an experimental RF signal direction finding payload in Low Earth Orbit (LEO). Successful outcome of this experiment could lead to significant benefits for the field of wildlife monitoring from Space. Commercial adoption of this process would enable the development and use of much smaller, lighter RF tracking tags, which in turn would considerably increase the potential range of species that could be tracked by Satellites.
The effect of the Covid-19 pandemic lockdowns has limited physical progress over the past 18 months, but the team continues to gain enormous experience and motivation from pursuing this exciting project with a very real-world mission. A recent return to near-normal working patterns has enabled the team to fully engage with the practicalities of progressing the previously produced WUSAT-3 Configuration Model, towards a testable Engineering Model.
This paper outlines the development of both the initial chassis prototype (including mechanisms) and a subsystem FlatSat as a first stage towards building the complete Engineering Model.
The chassis prototype was required to meet all the requirements of the FYS Design Specification [1], the NanoRacks CubeSat ICD [2], the CubeSat Design Specification [3] and those features identified by the outcomes of the WUSAT-3 Configuration Model.
The FlatSat was required to include all subsystems capable of being constructed and tested without the availability of certain proprietary items that will be purchased later. The function and interface of these items, where it was necessary for the purpose of testing the assembled subsystem units that were available, was met by the design and inclusion of temporary substitute arrangements that provided similar performance.
Systems Engineering methodologies were employed throughout as a means of ensuring that the design features of both chassis and FlatSat met all necessary requirements.

Keywords
CubeSat, Engineering-Model, FlatSat, Space, Systems,

[1] William Crofts, University of Warwick, United Kingdom, W.E.Crofts@warwick.ac.uk,
[2] University of Warwick, United Kingdom

Acronyms/Abbreviations

ADC	*Analogue-to-Digital Converter*
DDD	*Direct Displacement Damage*
DoD	*Depth of Discharge*
EEPROM	*Electrically Erasable Programmable Read-Only Memory*
EM	*Electromagnetic*
EPS	*Electrical Power System*
FlatSat	*Flat Satellite, internal subsystems of the satellite constructed and connected outside of the chassis*
FYS	*Fly Your Satellite*
LDO	*Low-Dropout*
LEO	*Low Earth Orbit*
OBDH	*On-Board Data Handling*
RF	*Radio Frequency*
SEE	*Single Event Effect*
SEU	*Single Event Upset*
TID	*Total Ionizing Dose*
TMR	*Triple Modular Redundancy*
WUSAT	*Warwick University Satellite*
XCAM	*The CubeSat Camera & Company*

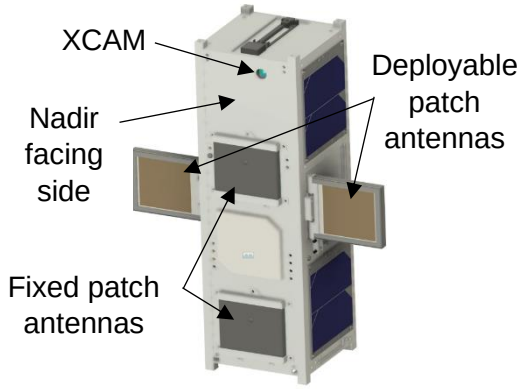

Figure 1. WUSAT-3 CubeSat Diagram

1. Introduction

In previous years, work carried out has been highly conceptual in nature, owing in no small part to the impact of the Covid-19 pandemic. Building upon the work of previous teams, the focus this year was translating conceptual designs into reality – manufacturing, assembling, and testing as many CubeSat subsystems as possible in preparation for the project's ambition of admission to the European Space Agency's Satellite Program [1].

2. Discussions

Detailed below is a summary of each subsystem developed this year by the WUSAT-3 team, outlining the key design features, their function, their testing and verification as well as relevant major considerations for each.

2.1 Chassis

The primary function of the chassis is to support the payload's ability to fulfill the satellite's mission. It provides a stable base to secure internal components during launch from Earth, as well as to withstand the vibrations and large forces experienced. The chassis consists of two side panels which incorporate four external rails, nadir and back panels, top and bottom plates alongside an additional internal structural support. The panels act as anchors to attach multiple patch antennas in addition to the solar panels required to power the system. Where required, cut outs were implemented to facilitate connections between external components and internal systems, with all designs conforming to the dynamic envelope specification [1].

2.2 Chassis Testing

Static stress testing was conducted using finite element software. Through Abaqus relevant parameters such as Von Mises stresses highlight areas which may be prone to yielding failures from loading and vibration during launch. This information has been used to inform design on key loadbearing components where reinforcement or redesign has been required. Additional simulation outputs investigated component deflection, which is presented as the displacement magnitude in Abaqus.

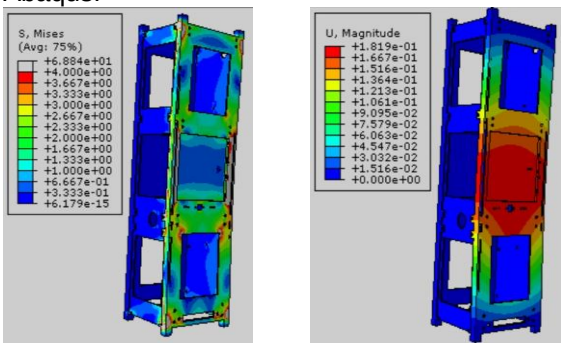

Figure 2. Results of simulation in Y axis showing the Von Misses stress in MPa (left) and deflection in mm (right)

The first simulation for stresses in the X axis shows values lie well within tolerated levels peaking at only 42.90 MPa. The maximum deflections of 0.04 mm are also well within reasonable safety margins. Similar results are seen across the Y axis with peak stress at 68.86

MPa causing a 0.18 mm deflection, and over the Z axis a peak 73.18 MPa resulted again in a small 0.18mm deformation. With the use of aluminium 7075 as the material for the chassis construction these forces are well below the 310 MPa yield limit.
Dynamic vibrational testing was also performed to gain insight on the natural frequency of the satellite chassis. This was carried out in similar fashion by simulation - with results yielding a first natural frequency 547.77Hz, which is well outside the required minimum tolerated 130Hz [1]. This testing however, indicated that large deformations of the structure up to 8.68mm could occur, which could potentially damage internal components, whilst also potentially exceeding the allowable dynamic envelope [1].

2.3 Internals

The internal components are separated into 'shelves', each containing a motherboard with the PC/104 form factor. Standoffs situated in the corners of each shelf, allow them to be arranged into a stack configuration across the axial length of the CubeSat, and maintain controlled separation between each internal component. This shelf stack fits within the chassis and is attached via the standoffs at two mounting points, located at the top and bottom plates respectively.

Figure 3. Configuration of Component Shelves

2.4 Patch Antenna Frame and Hinge

There are four payload patch antennas on the CubeSat (Abracon ARRTN5-915.000 MHz), each receiving data from the frequency of the RFID tags. Two are fixed and located on the nadir (Y+) panel of the satellite, and two are deployable from the side panels. The latter are constrained with a hinge to the X+ and X- panels respectively, where a deployment mechanism allows them to rotate 90° about the Y axis to face the Earth. Deployable antenna mechanisms were necessary, as there is insufficient space on the nadir panel to host all four of the earth facing antennas required by the payload – given the position of the camera aperture. Given the thickness of 6.9 mm of the antenna module, these could not be mounted flush onto the side panels of the chassis since it will exceed the maximum 6.5 mm of allowable dynamic envelope protruding from the side. Therefore, a recess in the aluminum chassis was implemented to house the patch antenna in its deployed configuration.

2.5 Deployment Mechanisms

The reliability of the deployment mechanisms for the patch and TM/TC antennas was a critical factor for guaranteeing the success of the WUSAT-3 mission. For this reason, the deployment mechanisms underwent rigorous design, testing and validation to ensure the designated mechanisms were sufficient. Both deployment mechanisms utilize a nichrome melt wire device to release the appropriate spring-loaded deployment mechanism for the respective antenna system. In order to increase the effectiveness of the burn wire break point, a spring mechanism pulls the melt wire in the direction of cutting across the respective burn wire. Collectively this mechanism is known as a "thermal knife".

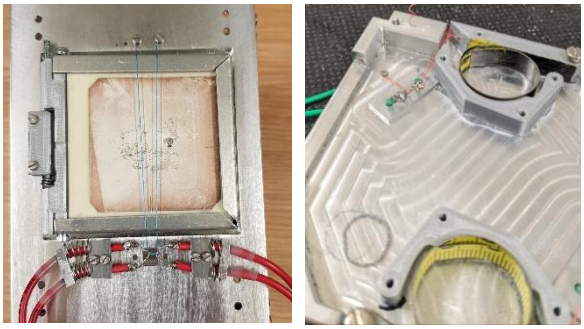

Figure 4. WUSAT Deployment Mechanisms

To reduce the likelihood of deployment failure – which would result in mission failure, redundant pairs of thermal knives were employed in the deployment mechanisms for each antenna. During testing, it was discovered that a sufficiently high current of 2.6 A would be required to ensure a successful cut within the acceptable time frame (< 10 seconds). For this reason, it would be necessary to activate only a single thermal knife at any given moment, to

remain within the limited power budget available from the satellite's battery. Thus, a sensor would be employed to detect unsuccessful antenna deployment and enable power to be re-routed to the redundant thermal knife. In addition, this design choice eliminates the possibility of burn wires becoming a source of space debris.

2.6 Thermal Radiation Considerations

Despite the abundance of literature about thermal radiation effects and shielding pertaining to CubeSats, there is a significant dearth of investigations into the effect of thermal radiation in space on the temperatures of internal electronic components. This lack of analysis seems strange – given that the internal electronics are the components for which a suitable temperature equilibrium must be maintained. For this reason, building on data obtained through previous thermal analyses, an investigation into the effects of thermal radiation – and specifically – how they affect the temperatures of internal electronics, was undertaken. The data yielded that, without insulation, the current design of the WUSAT-3 CubeSat would not be capable of sufficiently insulating its internal electronics, and that the minimum and maximum temperatures of at least one or several components would be exceeded in worst case, eclipse, or maximum solar flux scenarios.

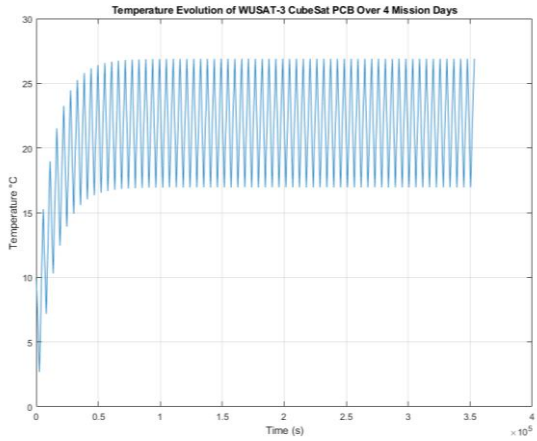

Figure 5. Internal Operation Temperature

This resulted in the implementation of aluminumized mylar multi-layer insulation within the interior of the chassis panels between the outer faces and the internal components. With the addition of this new insulation, results determined that the CubeSat would be capable of ensuring sufficient thermal stability for the duration of its deployment "survival" period, as well as the entire mission.

2.7 Electrical Power System (EPS)

Figure 6 illustrates the block diagram of the EPS, showing the basic layout for the power network. Power is generated by photovoltaic cells and subsequently transmitted to the EPS control, which includes components such as buck converters and additional subsystems to protect against under and over voltages. After this, the EPS control can proceed to distribute this power to the battery to charge it as well as to sensing subsystems within the CubeSat. The On Board Data Handling (OBDH) controls the EPS system and battery - distributing stored charge when needed and within the correct operating conditions. The battery outputs a range of voltages depending on the amount of remaining stored charge. In ideal conditions, it outputs 8.26 V DC, however this must still be reduced to a usable voltage for the range of components on the satellite. This is achieved with two buck converters; one to deliver regulated power to various subsystems and the other the delivered power to the OBDH microcontroller. These buck converters are a part of the power distribution in **Figure 6.** They were successfully designed, manufactured, and tested and are able to provide sufficient power to the satellite during operation.

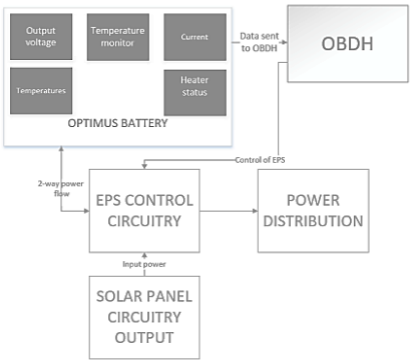

Figure 6. EPS Block Diagram

2.8 EPS Testing

The constructed buck converters, seen in **Figure 7Error! Reference source not found.**, were tested for their output voltages and their ripples to determine if they were suitable and could thus be accepted as feasible for further development. The LM22679 buck converter was found to successfully supply 5 V and 3.3V power rails for various subsystems, although outputs were measured at 5.2 V and 3.6 V respectively. The LM1036 buck converter delivers exactly 3.3 V to the microcontroller (PIC16), as desired. The ripple of all the power rails was found to be negligible due to the Low Dropout (LDO) regulators, names given respectively for each buck converter.

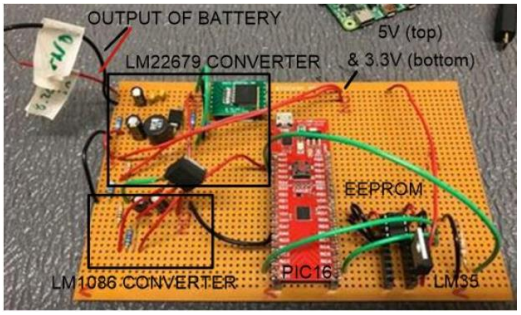

Figure 7. EPS Buck Converters and OBDH Components

2.9 On-Board Data Handling (OBDH) Coding

The OBDH is responsible for the data processing and storage needs of the various subsystems onboard. This includes coordinating, decoding, and executing telecommands received from the TM/TC component as well as providing the downlink data from the spacecraft. Therefore, the OBDH provides a platform for onboard subsystems and ground station to communicate with each other. Examples of operations the OBDH would perform include, processing sensor data such as temperature and voltage, and ensuring the system is in a safe operating window. Another example would be to send a command to the camera system to take a picture, process it and then transmit it to the ground via the S-Band payload downlink system. Most recently, work was undertaken to realise simulations of the I^2C, Digital and Analogue protocols and subsequently to connect it to the EPS and verify the function of both subsystems. These protocols will provide the foundations of the OBDH and allow further work to focus on the operation of the satellite.

2.10 OBDH Code Verification

Code for the I^2C, digital and analogue protocols was successfully written and tested with the chosen microcontroller, PIC16F15376. The I^2C protocols were tested with the PIC16, by writing 'WUSAT' in ASCII to an EEPROM, non-volatile memory, which was then removed and read by an Arduino MEGA using a serial monitor to read the addresses. The analogue and digital protocols were tested by using the analogue-to-digital converter (ADC), in the PIC16, by taking the analogue output of a temperature sensor (LM35) and converting it to a digital 10-bit reading, to then be stored in the EEPROM. Both tests were successful, confirming the successful function of the protocols' code.

The temperature sensor test was repeated on the EPS board in **Figure 7**, but an unknown source of error meant that random noisy readings compromised results for 40 seconds. After this initial settling period, the readings were as expected.

2.11 Battery

After a critical design review, it was decided that it was necessary to use a commercially sourced battery to ensure battery suitability for crew-rated missions. The Clyde Space Optimus battery was selected due to its flight heritage and features such as the on-board current and voltage measurements which can communicate via I^2C to the OBDH as well as integrated heaters [2]. The battery size, however, was not yet justified with respect to the power budget. The battery chosen is the 40Wh as this is large enough to sustain the operation of the satellite whilst in eclipse.

2.12 Camera

Located at the top of the nadir panel, the C3D CubeSat camera board from XCAM was selected to fulfil the Earth imaging requirements of the WUSAT 3 mission. The reasons for its selection include previous flight heritage of the design, adherence to standard CubeSat dimensions and stacking connections and the offer from XCAM of the donation of a C3D board for the WUSAT 3 mission.

2.13 XCAM Camera Emulation

Figure 8 shows the camera emulation created to emulate the function and operation of the XCAM camera system. It uses I^2C protocols [3], just as the real camera would, to send the image to the microcontroller. The model was tested successfully, with a connected computer receiving the image taken by the Raspberry Pi camera (left). A limitation of the XCAM system is its use of volatile memory, which increases the power consumption of the satellite.

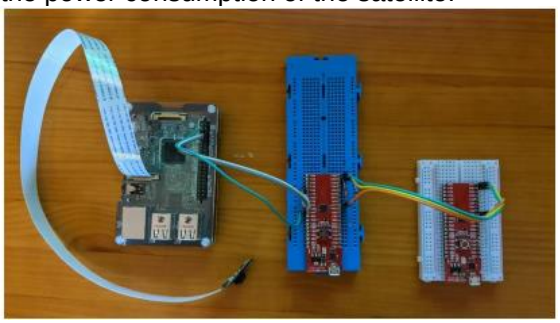

Figure 8. XCAM Stand In

2.14 Attitude Determination and Control System (ADCS)

To confirm which configuration of ADCS would be the most optimal for fulfillment of mission requirements, simulation data provided by CubeSpace Ltd allowed for the model

specification as well as selection of optional components to be determined. From this data, the Y-Momentum CubeADCS model was selected for implementation in the CubeSat. [4]. This item will be purchased when funds are available.

2.15 Electromagnetic (EM) Radiation Considerations

Electromagnetic radiation is of significant concern to satellite engineers, particularly given the small size of the WUSAT-3 CubeSat and the potential options for shielding. For this reason, an investigation into EM radiation effects on onboard silicon devices was undertaken, using industry standard modelling toolkit – SPENVIS. Given relevant mission and design parameters, it was determined that the effects of persistent radiation such as Total Ionizing Dose (TID) and Direct Displacement Damage (DDD), were not of significant concern given the planned thickness of aluminum shielding (**Figure 9**). Over the course of the entire mission, the expected TID was determined to be just 100 rad – significantly below the dangerous limit for silicon devices of 10-25 krad.

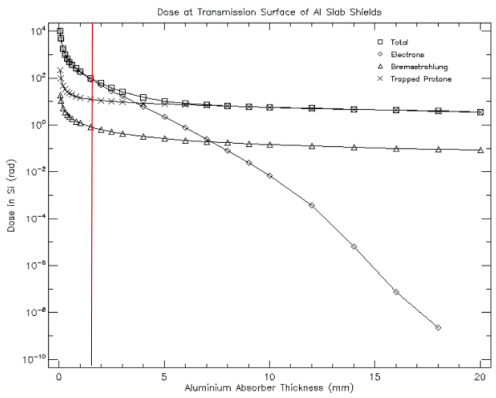

Figure 9. TID with varying Al Shielding Thicknesses

Transient radiation, such as Single Event Effect (SEE), warranted more significant concern and required specific mitigation, as the total number of expected bitflips within transistors was determined to be 896 for the duration of the mission. As this could lead to disruption of communications or data corruption in the OBDH, triple modular redundancy (TMR) was implemented to alleviate the threat posed.

Following a review of potential EM radiation counter measures, an altered version of TMR was chosen. This altered TMR will act as a data storage device and the majority voter with the microcontroller used for the on-board data handling, as seen in **Figure 10**. The PIC16 will read the data in each of the devices, using I^2C, and determine the majority response. In doing this, it will also be able to replace any discrepancies between the data devices. The trade-off will be minor as the data storage, EEPROMs are very light weight (1g), compact (under $1cm^3$), low power (17.5µW) and each can store 1Mb so they can easily be integrated into the system. The limiting factor of this design is if the PIC16's bandwidth is sufficient to process comparative commands on top of monitoring the satellite's vitals and other on-board data, which all rely on the amount of RAM available.

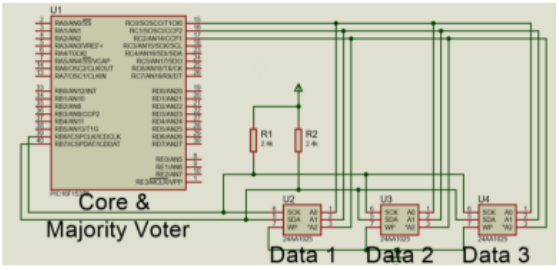

Figure 10. Altered TMR Schematic

By designing the electronic architecture to incorporate three parallel cores and a majority voter system, the probability of an SEU simultaneously corrupting data values within multiple voters – and then propagating this error into the data handling system – is significantly reduced. With the implementation of TMR – the expected number of bit flips over the mission, is reduced to just 1.68 - a reduction of 99.8%.

3 Conclusions

This work represents a sizeable leap forward in moving WUSAT-3 development towards an Engineering Model ready for testing. The integrated work of the WUSAT-3 team has produced a number of working subsystem units that will allow rapid development to the next stage.

4 References

[1] ESA. FYS4! Programme Website. ESA - Fly Your Satellite! programme Last visited: 20th March 2022

[2] Clyde Space, Optimus Datasheet, Website. AAC_DataSheet_Optimus.pdf (aac-clyde.space) last visited 23rd February 2022

[3] XCAM, C3D Camera, Website. C3D CUBESAT CAMERA | XCAM last visited 14th January 2022

[4] CUBESPACE ADCS Website. Documentation & CAD | CubeSpace last visited 18th March 2022